Article

Ultraviolet-Initiated Decomposition of Solid 1,1-Diamino-2,2-dinitroethylene (FOX-7)

Andrew M. Turner, Joshua H. Marks, Jasmin T. Lechner, Thomas M. Klapötke, Rui Sun, and Ralf I. Kaiser*

Read Online

ACCESS | 📊 Metrics & More | 📖 Article Recommendations | 🆂�ᵢ Supporting Information

ABSTRACT: FOX-7 (1,1-diamino-2,2-dinitroethylene) was photolyzed with 202 nm photons to probe reaction energies, leading to the decomposition of this energetic material and to compare results from irradiations using lower-energy 532 and 355 nm photons as well as higher-energy electrons. The photolysis occurred at 5 K to suppress thermal reactions, and the solid samples were monitored using Fourier transform infrared spectroscopy (FTIR), which observed carbon dioxide (CO_2), carbon monoxide (CO), cyanide (CN^-), and cyanate (OCN^-) after irradiation. During warming to 300 K, subliming products were detected using electron-impact quadrupole mass spectrometry (EI-QMS) and photoionization time-of-flight mass spectrometry (PI-ReTOF-MS). Five products were observed in QMS: water (H_2O), carbon monoxide (CO), nitric oxide (NO), carbon dioxide (CO_2), and cyanogen (NCCN). The ReTOF-MS results showed overlap with electron irradiation products but also included three intermediates for the oxidation of ammonia and nitric oxide: hydroxylamine (NH_2OH), nitrosamine (NH_2NO), and the largest product at 76 amu with the proposed assignment of hydroxyurea ($NH_2C(O)NHOH$). These results highlight the role of reactive oxygen intermediates and nitro-to-nitrite isomerization as key early reactions that lead to a diverse array of decomposition products.
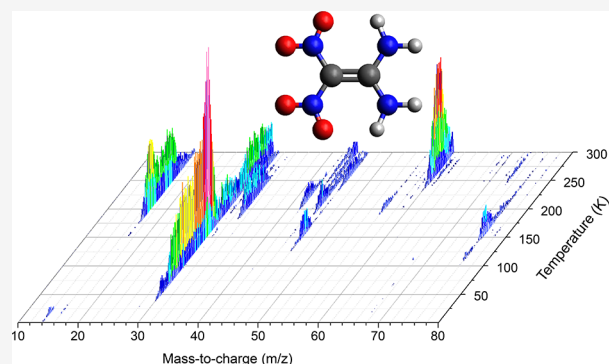
1. INTRODUCTION

1,1-Diamino-2,2-dinitroethylene (FOX-7) represents a next-generation energetic material to replace current explosives such as 1,3,5-trinitro-1,3,5-triazinane (RDX), octahydro-1,3,5,7-tetranitro-1,3,5,7-tetrazocine (HMX), and conventional trinitrotoluene (TNT).[1−4] These energetic materials, along with CL-20 (hexanitrohexaazaisowurtzitane) and octanitrocubane are cyclic compounds possessing nitro ($-NO_2$) groups,[5,6] while a FOX-7 molecule (Scheme 1) is acyclic and contains amino groups ($-NH_2$) along with nitro groups. For FOX-7,

Scheme 1. 1,1-Diamino-2,2-dinitroethylene (FOX-7)
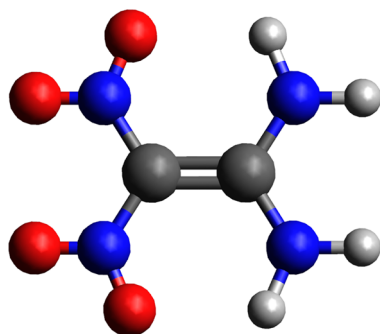
these molecular differences contribute to a distinct variety of reaction products that provide critical information for an understanding of the decomposition mechanisms. Such information is necessary to fully evaluate the sensitivity, efficiency, stability, and safety of energetic materials.[7−12] The study of the underlying reaction pathways is complicated by carbon-, oxygen-, and nitrogen-centered radicals and unstable reaction intermediates born from a complex nonequilibrium chemistry, leading to first-generation products that may rapidly react to form higher-order products.[13,14] Considering these difficulties, computational studies often investigate the decomposition of energetic materials, while experimental results complement but very often contradict theoretical predictions. Such is the case for FOX-7, with several conflicting computational and experimental results presenting an unclear picture of FOX-7 decomposition pathways.[15−20]
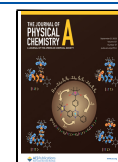
A key initial decomposition step involves the nitro-to-nitrite isomerization[21] with a 245 kJ mol^{-1} isomerization barrier.[16,18] Experiments have shown the cleavage of the newly formed O—NO bond generates nitric oxide (NO),[21] while subsequent decomposition leads to hydrogen isocyanide (HNC) and carbon monoxide (CO).[16] Another prominent initial reaction step breaks the C—NO$_2$ bond, which is much weaker (280–301 kJ mol^{-1})[15,18,22–25] than the C—NH$_2$ bond (461–503 kJ mol^{-1}),[15,21–23] and this produces nitrogen dioxide (NO$_2$).[26] These initial steps exhibit a temperature dependence such that breaking the C—NO$_2$ bond is preferred over the nitro-to-nitrite isomerization above 250 K.[27] A hydrogen shift from the amine group (—NH$_2$) to the nitro group (—NO$_2$), followed by C—NO$_2$ bond cleavage results in nitrous acid (HONO).[16] Although this hydrogen shift is not predicted in the gas phase, it is a significant step in solid-state decomposition.[28] Since calculations consider predominantly only a single gas-phase FOX-7 molecule, the influence of the solid matrix has often been overlooked even though FOX-7 experiences intermolecular hydrogen bonding that affects the reaction energies and, hence, reaction mechanisms of decomposition.[17,29]

Thermal decomposition of solid FOX-7 above 500 K produces carbon monoxide (CO), carbon dioxide (CO$_2$), ammonia (NH$_3$), hydrogen cyanide (HCN), cyanic acid (HOCN), isocyanic acid (HNCO), formic acid (HCOOH), water (H$_2$O), nitric oxide (NO), nitrogen dioxide (NO$_2$), nitrous acid (HONO), nitrous oxide (N$_2$O), and dinitrogen trioxide (N$_2$O$_3$).[30,31] In such cases, hydroxyl radicals (OH) and NO$_2$ were found to abstract hydrogen to generate H$_2$O and HONO.[32] At elevated temperatures, α-FOX-7 transitions to a β-phase above 385 K and eventually to γ- and δ-FOX-7 before thermally decomposing.[17,18,28–31,33–36] Recently, ε- and ζ-phases have also been synthesized that convert to a γ-phase upon heating.[37] Although subtle changes were observed in the infrared spectrum upon cooling to cryogenic temperatures under vacuum, a distinct low-temperature phase has not been observed.[17] While different reaction characteristics are observed among the various phases, changes due to deuteration of FOX-7 were found to affect only the α-phase but not the γ-phase.[38]

Recently, research into energetic materials has expanded to mixing FOX-7 with energetic constituents and utilizing FOX-7 as a model compound while studying various derivatives to improve explosion and handling characteristics. FOX-7 has been theoretically investigated mixed with 2,3,5,6-tetra(1H-tetrazol-5-yl)pyrazine (H$_4$TPP)[39] and experimentally mixed with CL-20 and HMX that resulted in greater thermal and shock stability.[36,40] In addition, nanosized FOX-7 was mixed with zeolitic imidazolate framework-8 (ZIF-8), which resulted in a catalyzed decomposition with less mechanical sensitivity.[41] FOX-7 was reacted with bases such as hydrazine (N$_2$H$_4$), hydroxylamine (NH$_2$OH), ammonia (NH$_3$), pimagedine (NH$_2$C(NH)NHNH$_2$), and inorganic hydroxides (OH$^-$) to form energetic salts with propulsive and detonation characteristics superior to RDX.[42] Derivatives of FOX-7 have also provided additional insight into decomposition mechanisms. By increasing the amine group (—NH$_2$) to a multinitrogen amine chain, NO$_2$ and HONO were produced by a distinct method to that of FOX-7.[43] Computational and solution studies of diazacylic derivatives of FOX-7 found similar initial decomposition pathways as FOX-7 but were in disagreement in the solid state due to catalytic products generated in the partially liquefied samples.[44,45] A computational study that replaced the central carbon–carbon double bond of FOX-7 with various nitrogen-containing heterocycles found improved detonation characteristics with higher nitrogen content.[46] A similar study with a four-membered heterocyclic ring inserted into the carbon–carbon double bond of FOX-7 showed lower impact sensitivity with good detonation parameters.[47]

While computational studies often consider the energetics and decomposition mechanisms for individual reactions, purely experimental investigations of FOX-7 usually focus on bulk properties, and thus molecular-scale computational findings rarely reconcile with experiments. Here, we present experimental results of the 202 nm photon-initiated decomposition of solid FOX-7 at 5 K that extends a systematic investigation of previously reported irradiations using 532 and 355 nm photons[17] along with energetic electrons in order to elucidate how molecular decomposition processes relate to the impinging energy and reaction energetics.[48] The 532 nm photolysis only generated a small quantity of molecular oxygen (O$_2$), while 355 nm photolysis produced four times greater molecular oxygen (O$_2$) along with nitric oxide (NO). Utilizing electronic structure calculations, these photolysis experiments probe the individual mechanisms involved in FOX-7 decomposition by limiting the photon energy to discrete values capable of overcoming calculated reaction barriers to compare predicted products with experimental results. In addition to targeted photolysis studies, solid FOX-7 was previously irradiated with low-energy electrons generated in the wake of energetic electrons with the largest products having a mass-to-charge ratio (m/z) of 96, which was assigned to C$_3$N$_2$O$_2$ and the proposed isomer of cyano(oxo)methyl cyanate (NCC(O)OCN).[48] No molecular oxygen was observed, but instead, the terminal oxidation products carbon monoxide (CO), carbon dioxide (CO$_2$), and nitrogen dioxide (NO$_2$) formed, which were absent in the 532 and 355 nm photolysis studies. Thus, an investigation utilizing 202 nm photolysis provides an intermediate energy between 355 nm photons and electron irradiation capable of accessing discrete intermediates associated with the fate of oxygen eventually locked up in the "terminal" oxidation products (CO, CO$_2$, NO$_2$). The photolysis products that remain in the solid were observed using Fourier transform infrared spectroscopy (FTIR) while subliming products, either during irradiation or heating to 300 K, were monitored using two mass spectrometry methods: electron-impact quadrupole mass spectrometry (EI-QMS) and the more sensitive photo-ionization reflectron time-of-flight mass spectrometry (PI-ReTOF-MS). The results are compared to those from lower-energy photolysis and higher-energy electron irradiation to illuminate the energetics required to achieve various reaction products.

2. EXPERIMENTAL SECTION

FOX-7 was synthesized[17] according to procedures described by Latypov et al.[49] and Astrat'ev et al.,[50] and thin polycrystalline films with a thickness of 2.0 ± 0.3 μm were prepared on polished silver substrates by dispensing dropwise a dilute solution of FOX-7 in dimethyl sulfoxide (DMSO) and evaporating under vacuum. The nature of the waved sheets that compose condensed FOX-7 has been described previously.[17] Experiments were performed in a stainless steel ultrahigh vacuum (UHV) chamber evacuated to less than 1 × 10^{-10} Torr.[51,52] Within the experimental chamber, the

substrates were affixed to copper cold finger cooled by a two-stage helium refrigerator (Sumitomo Heavy Industries) to 5.0 ± 0.1 K. After cooling to 5 K, the sample was annealed to 320 K to remove residual DMSO from the FOX-7 matrix and then returned to 5 K. The sample was irradiated with 202 nm photons (10 mW cm^{-2}, 1.0 × 10^{16} photons s^{-1} cm^{-2}) generated by tripling the 606 nm output of a dye laser utilizing a Rhodamine 610/640 dye solution pumped by the second harmonic (532 nm) of an Nd:YAG laser (Spectra Physics PRO 250, 30 Hz). During photolysis, Fourier transform infrared (FTIR) spectra were collected using an external Thermo Nicolet 6700 along a dry nitrogen-purged beam path that passes into and out of the UHV chamber using differentially pumped potassium bromide (KBr) windows. The infrared beam interacts with the sample through absorption—reflection—absorption at a 44° angle of incidence and is recorded using an external liquid nitrogen-cooled mercury—cadmium—telluride type-B (MCT-B) detector.[5,17,48,51] After 2.5 h of irradiation, the sample was warmed to 320 K at 1 K min^{-1} as a temperature-programmed desorption (TPD) protocol. During TPD, subliming molecules were detected using photoionization reflectron time-of-flight mass spectrometry (PI-ReTOF-MS, Jordan TOF Products) utilizing 10.49 eV photons generated by tripling the third harmonic (355 nm) of the Nd:YAG laser using nonresonant four-wave mixing ($\omega_2 = 3\omega_1$) with pulsed xenon gas as the nonlinear medium.[53] The photoion signals were amplified (Ortec 9305) and recorded by a FAST ComTec MCS6A multichannel scalar operating at 30 Hz (Quantum Composers 9518). In addition, electron-impact (EI, 70 eV) quadrupole mass spectrometry (QMS) monitored the residual gases during irradiation and TPD, which was useful for detecting compounds with ionization energies (IEs) greater than 10.49 eV that would not be observed using PI-ReTOF-MS. In order to confirm mass spectral assignments, isotopically labeled samples were prepared by dissolving deuterated FOX-7 (d4-FOX-7)[54] in deuterated DMSO under a sealed nitrogen atmosphere to limit hydrogen exchange, which was prevalent in solution under ambient air. However, the dried thin film was found to be inert to hydrogen exchange. In addition, blank experiments without irradiation were performed to ensure any observed products and changes to FOX-7 were only caused due to the irradiation.

3. RESULTS

3.1. Infrared Spectroscopy. The infrared spectra taken before and after irradiation (Figure 1 and Table S1) display similar decreases across all FOX-7 peaks and contain new product peaks from 2000 to 2400 cm^{-1} (Figure 1, bottom). The decrease in intensity of the vibration bands associated with functional groups of FOX-7, such as C=C (ν_9), −NH (ν_1−ν_4), and −NO$_2$ (ν_{10}),[17] are shown in Figure 2 and indicate that 81.5 ± 1.0% of FOX-7 remains after irradiation. The decline generally follows a pseudo-first-order decay with rate constants of $k_{C=C} = 2.4 \times 10^{-5}$ s^{-1}, $k_{NH} = 2.3 \times 10^{-5}$ s^{-1}, and $k_{NO_2} = 2.1 \times 10^{-5}$ s^{-1}. These rate constants indicate similar decomposition rates between functional groups. In contrast, the rate constants from electron irradiation ($k_{C=C} = 6.8 \times 10^{-4}$ s^{-1}, $k_{NH} = 2.1 \times 10^{-3}$ s^{-1}, and $k_{NO_2} = 1.3 \times 10^{-3}$ s^{-1})[48] display greater variance between their values—a 1:3:2 ratio—and are 30 to 90 times larger in magnitude than the rate constants from 202 nm photolysis. Unlike the infrared signals from electron irradiation,[48] which showed an asymptotic behavior as the
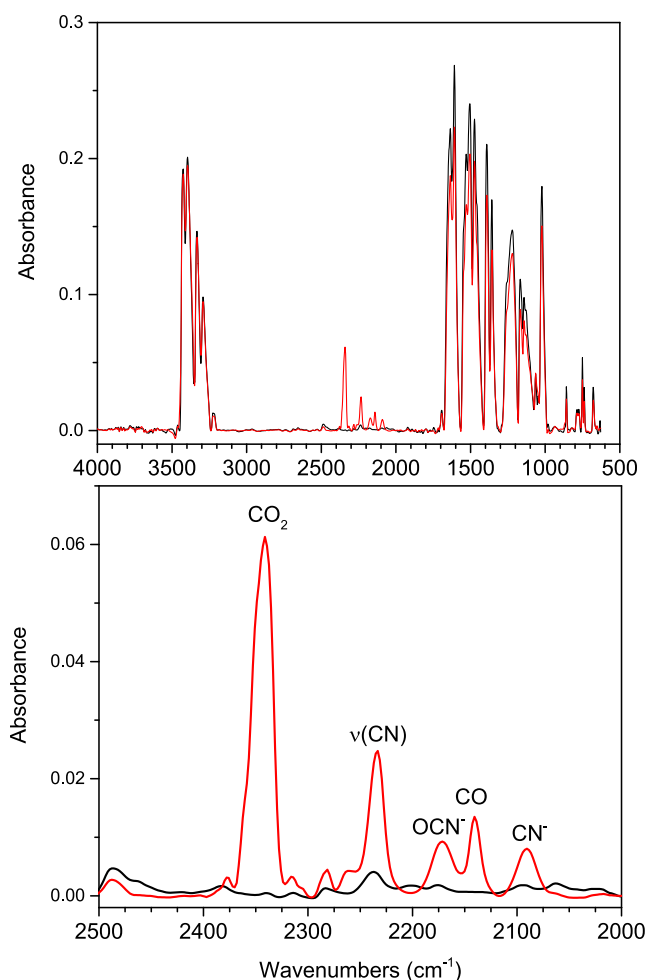
Figure 1. Infrared spectra of solid FOX-7 collected before (black) and after (red) irradiation at 5 K.

uppermost 320 nm FOX-7 layer decomposed, the spectra from 202 nm irradiation show no such behavior, suggesting that the FOX-7 sample transmits a large portion of the irradiation and the sample is processed at all depths. Based on the number of reacted molecules and the photon flux, 300 photons impinged the sample on average for every reacted molecule. Assuming that multiphoton processes are absent and that the absorption of one photon results in the decomposition of one molecule, this indicates FOX-7 is largely transparent to 202 nm photons, which is consistent with previously recorded UV−vis spectra of solid FOX-7 that show diminishing absorption strength at energies higher than the 395 nm peak.[17]

Two neutral products were observed in the infrared spectrum after irradiation: carbon dioxide (CO$_2$) at 2341 cm^{-1} and carbon monoxide (CO) at 2141 cm^{-1}. In addition, two ionic species were identified including cyanide (CN$^-$, 2090 cm^{-1}) and cyanate (OCN$^-$, 2171 cm^{-1}), and the C≡N stretching of the nitrile functional group (ν(CN)) was assigned to 2233 cm^{-1}. Using the integrated absorption coefficients for the molecular and ionic species (CO$_2$, 7.3 × 10^{-17} cm molecule^{-1}; CO, 1.1 × 10^{-17} cm molecule^{-1}; CN$^-$, 3.7 × 10^{-18} cm molecule^{-1}; OCN$^-$, 1.3 × 10^{-16} cm molecule^{-1}), the column densities for each species (i.e., the number of molecules per cm^2 along the line of sight of the infrared beam) were calculated and temporal profiles (Figure 3) were obtained during irradiation. Cyanide is the most abundant
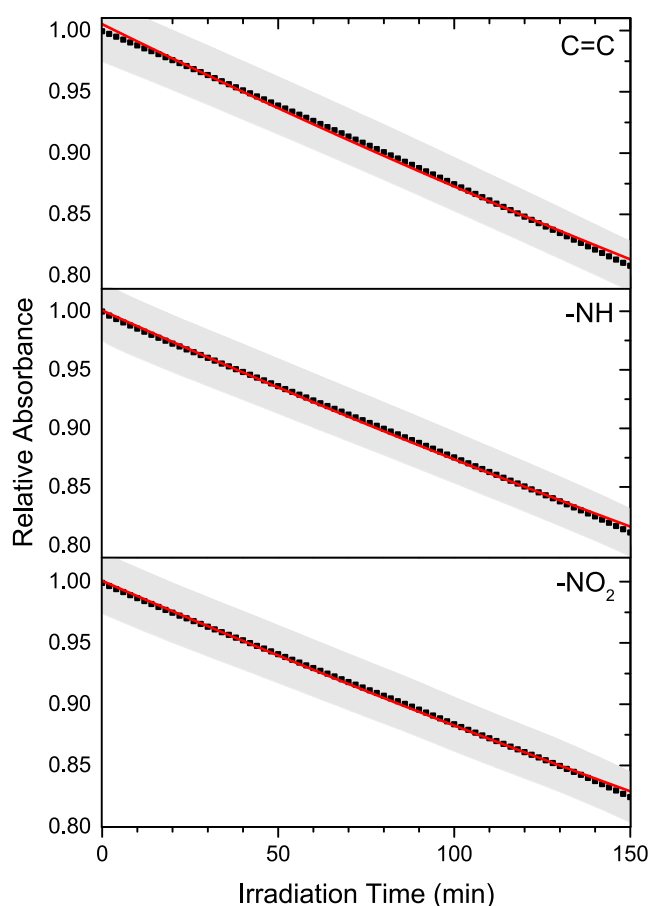
Figure 2. Infrared intensities for three functional groups of FOX-7 (C=C, −NH, and −NO₂) relative to their pre-irradiation starting values. The plots show that about 81.5% of the functional groups remain after irradiation. Red lines indicate fitting using first-order rate constants.

product observed after irradiation (1.2×10^{16} molecules), followed by carbon dioxide (5.8×10^{15} molecules), carbon monoxide (3.2×10^{15} molecules), and cyanate (3.3×10^{14} molecules). Considering that $18.5 \pm 1.0\%$ of the $2~\mu m \times 1~cm^2$ layer reacted and using the density of FOX-7 of 1.89 g cm⁻³, $2.8 \pm 0.7 \times 10^{17}$ molecules of FOX-7 were photolyzed. Equating this to 5.7×10^{17} carbon atoms and comparing to the species trapped in the matrix after irradiation, 2.1% of the reacted carbon produced cyanide, 0.6% produced carbon dioxide, 0.3% formed carbon monoxide, and only 0.03% resulted in cyanate. Thus, only 3% of the reacted carbon is accounted for by small molecules in the infrared spectra, with the remaining carbon likely remaining in the solid matrix as a variety of partially reacted species. The temporal profiles for these four product peaks (Figure 3) display an initial exponential rise that becomes linear by the latter portion of the irradiation, indicating that the photolysis is still in the early stages as production has yet to diminish.

3.2. Quadrupole Mass Spectrometry. Ion signals for five species were observed during TPD using quadrupole mass spectrometry: $m/z = 18, 28, 30, 44,$ and 52 (Figure 4). Four of these signals were observed at the same mass-to-charge ratio (m/z) in the d4-FOX-7 experiments, $m/z = 28, 30, 44,$ and 52, indicating that the products associated with these ion counts have no hydrogen atoms. The final signal at $m/z = 18$ matched the TPD profile of $m/z = 20$ for d4-FOX-7, signifying that this product has two hydrogen atoms. Thus, the assignments are water (H_2O, $m/z = 18$), carbon monoxide (CO, $m/z = 28$), nitric oxide (NO, $m/z = 30$), carbon dioxide (CO_2, $m/z = 44$), and cyanogen (NCCN, $m/z = 52$). Carbon monoxide was assigned to $m/z = 28$ instead of dinitrogen (N_2) because the $m/z = 12$ signal of C⁺ follows the $m/z = 28$ trace, indicating a carbon-containing species. The TPD profile of water presents as a single sublimation event starting at 150 K and peaking at 172 K. The other four molecules detected by QMS also have corresponding peaks at this temperature, indicating that a portion of these molecules were bound to water and were
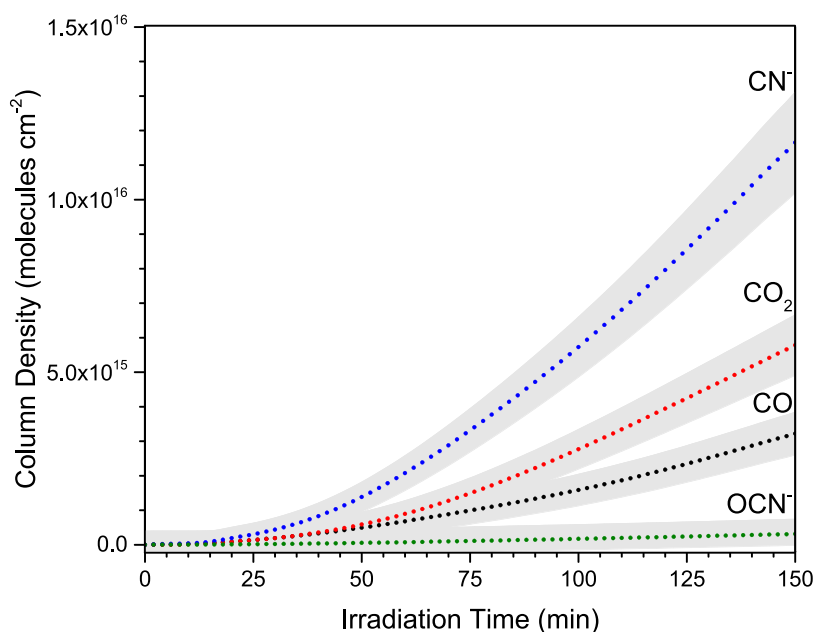
Figure 3. Column densities of carbon dioxide (CO₂, red), carbon monoxide (CO, black), cyanide (CN⁻), and cyanate (OCN⁻) within the FOX-7 sample during irradiation.
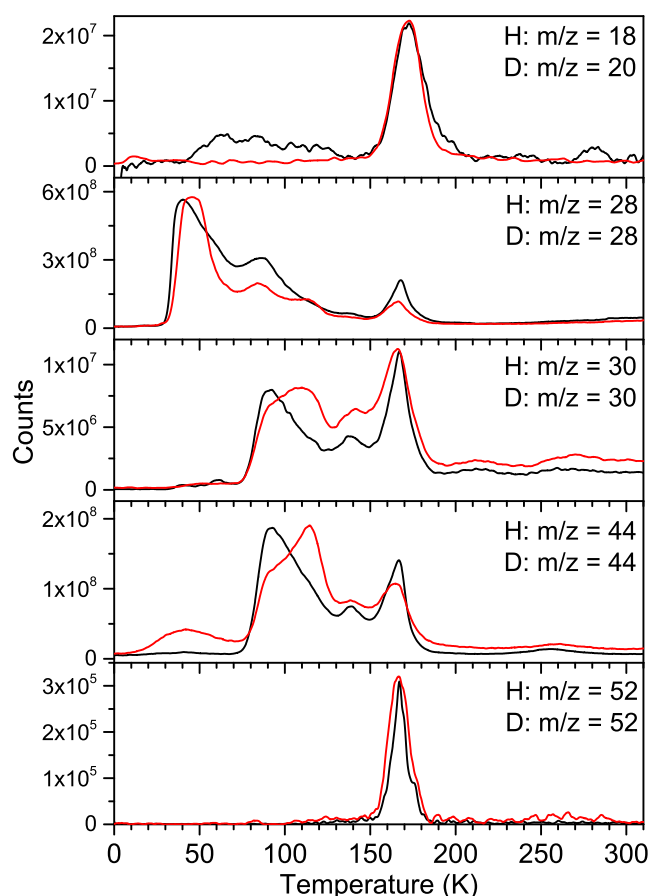
Figure 4. TPD sublimation profiles recorded using QMS showing signals at mass-to-charge ratios (m/z) based on FOX-7 with hydrogen ("H," red) and deuterium ("D," black). The scale indicates the counts observed for H-FOX-7.

released during water sublimation. Carbon monoxide has the lowest sublimation temperature observed, beginning at 28 K and peaking at 42 K. Additional peaks occurred at 85 K, which is during NO and CO_2 sublimation, and during H_2O sublimation at 168 K, which suggests that CO was weakly bound to these products and co-sublimed during their initial sublimation. This suggests CO must overcome approximately 20 and 50 kJ mol^{-1} additional binding energy to sublime with NO/CO_2 and H_2O.[55] Each sublimation peak of CO occurs at the same temperature in the FOX-7 and d4-FOX-7 samples, and variations in intensity are simply due to differences in the sample matrix.

The TPD profiles for NO ($m/z = 30$) and CO_2 ($m/z = 44$) are similar: both began subliming at 75 K, passed through a shoulder at 90 K to a peak at 112 K (this shoulder and peak designation are reversed in the d4-FOX-7 experiments), had a small peak at 138 K, and finished with a peak at 168 K. The similarity between the $m/z = 30$ and 44 profiles suggests a connection between these signals, such as a compound with $m/z = 44$ fragmenting to the lower-intensity (1:20 signal ratio) $m/z = 30$. Since the profiles do not exactly match, two compounds could contribute to the $m/z = 44$ signal, one of which fragments to NO, or NO may also have formed during irradiation and supplement any fragmentation signal. Besides CO_2, nitrous oxide (N_2O) has a mass-to-charge ratio of 44 without hydrogens, and N_2O can fragment to NO. To confirm the assignment for $m/z = 44$, the TPD profile for $m/z = 45$ was

compared to the expected isotopic distribution of CO_2 and N_2O with carbon-13 (1.08%), nitrogen-15 (0.36%), and oxygen-17 (0.04%).[56] Figure S1 demonstrates that the signal for $m/z = 45$ can be entirely explained by $^{13}CO_2$ without the need for N_2O, and the primary sublimation event with a 75 K onset is consistent with the sublimation temperature of pure CO_2 ice.[57] Additionally, the $m/z = 30-44$ fragmentation ratio for nitrous oxide using electron-impact QMS is 1:3,[58] which is far greater than the 1:20 ratio observed between these TPD profiles and further supports the nonassignment of N_2O to $m/z = 44$. Instead, this signal belongs to CO_2, while NO at $m/z = 30$ co-sublimed, creating similar TPD profiles. The final signal observed using QMS was cyanogen at $m/z = 52$. The TPD profile has a single sublimation peak beginning at 150 K and peaking at 167 K in a manner similar to the profile of H_2O.

Previous experiments of electron-irradiated FOX-7 detected the same five compounds using QMS. This is in contrast with lower-energy photon irradiation at 355 and 532 nm, which only observed nitric oxide (NO) and molecular oxygen (O_2) as products. However, O_2 was not detected from 202 nm irradiation, but instead, the combustion products of carbon-containing molecules—CO and CO_2—were produced, highlighting a critical energy difference between 202 and 355 nm photons capable of supplying sufficient energy not only to generate oxygen atoms but to proceed with higher-order reactions involving these oxygen atoms. The electron irradiation also imparted excess energy to the sample, such that most of the gas-phase products were detected by QMS during irradiation and not during TPD. In contrast, a negligible quantity of products degassed from the sample during 202 nm irradiation, and instead, the products were observed during TPD. By depositing known quantities of CO_2 or NO ices and utilizing ionization cross sections, previous experiments[48] performed QMS calibrations that reported conversion factors (K) between the number of detected molecules and the number of molecules that had sublimed. The factors for these five products are $K_{H_2O} = 6.5 \times 10^5$, $K_{CO} = 5.8 \times 10^5$, $K_{NO} = 4.2 \times 10^5$, $K_{CO_2} = 5.0 \times 10^5$, and $K_{NCCN} = 3.5 \times 10^5$, meaning one in every 3.5×10^5 molecules of NCCN that sublime from the sample is detected by QMS. The most abundant molecule detected by QMS was carbon monoxide, with 1.9×10^{16} molecules subliming from the sample. This value accounts for the fragmentation of CO_2 to CO by QMS, which resulted in a $m/z = 28$ signal that was 8% of the $m/z = 44$, and thus the carbon monoxide quantities were corrected for this. After carbon monoxide, carbon dioxide was the next most abundant species with calculated 6.0×10^{15} gas-phase molecules. This value is in excellent agreement with the number of CO_2 molecules detected after irradiation using FTIR (5.8×10^{15}). However, the QMS results indicate that six times greater amounts of CO sublimed from the sample than were detected by the FTIR after irradiation (3.2×10^{15}). This suggests that irradiated FOX-7 released additional carbon monoxide in the warm-up phase. Much lower quantities of water (6.5×10^{14} molecules), nitric oxide (2.5×10^{14} molecules), and cyanogen (1.4×10^{12}) were calculated using the QMS results. Although large quantities of cyanide were observed in the infrared spectrum after irradiation, in the TPD phase, this did not translate to large amounts of cyanogen or other cyano-containing compounds, such as hydrogen cyanide (HCN), and thus most of the cyanide generated by irradiation remained in the solid sample. Using the QMS data for CO, CO_2, and
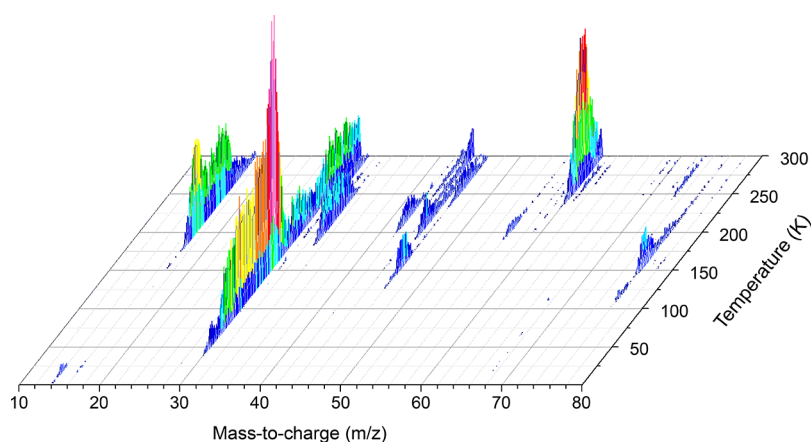
Figure 5. ReTOF-MS signals of irradiated FOX-7 during TPD for $m/z = 10-80$.
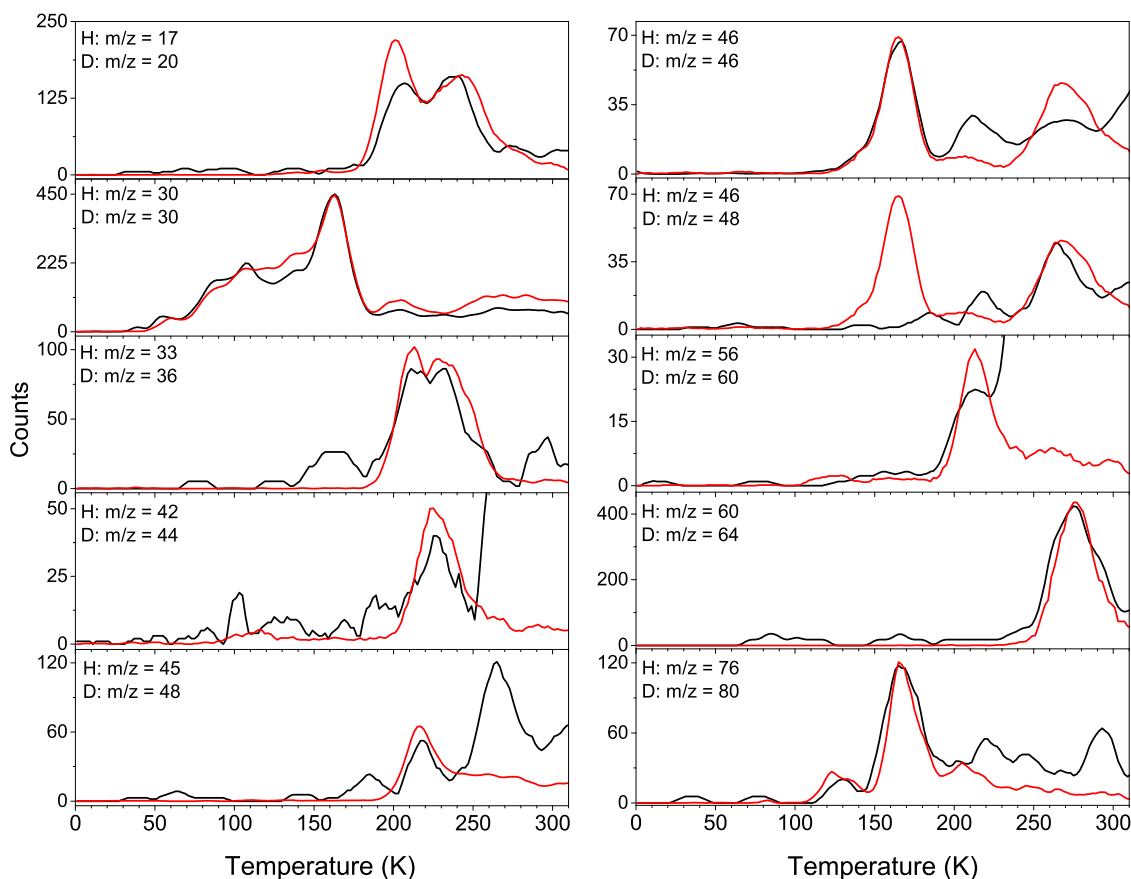
Figure 6. TPD profiles for signals recorded using ReTOF-MS showing signals at mass-to-charge ratios (m/z) based on FOX-7 with hydrogen (H, red) and deuterium (D, black). The scale indicates the counts observed for H-FOX-7.

NCCN, 2×10^{16} carbon atoms sublimed from the FOX-7 sample, leaving 97% of the 5.7×10^{17} reacted carbon atoms remaining in the solid state.

3.3. Reflectron Time-of-Flight Mass Spectrometry. After irradiation, subliming molecules were also monitored during the TPD phase with ReTOF-MS utilizing 10.49 eV photons for photoionization (Figures 5 and 6). While ReTOF-MS is a more sensitive method than QMS, this ReTOF-MS method is limited to molecules with ionization energies (IE) less than 10.49 eV. Thus, H_2O (IE = 12.62 eV), CO (IE = 14.01 eV), CO_2 (IE = 13.78 eV), and NCCN (IE = 13.37 eV), which were observed in QMS, cannot be detected using 10.49

eV photons. Furthermore, compounds that might be expected from the FTIR spectra, such as hydrogen cyanide (HCN, IE = 13.6 eV)[58] and cyanic acid (HOCN, IE = 11.9 eV) or isocyanic acid (HNCO, IE = 11.6 eV)[59] would not be detected. However, nitric oxide (NO, IE = 9.26 eV, $m/z = 30$) was observed and began subliming at 33 K and passed through several lower-intensity regions before peaking with water sublimation at 162 K. The matching TPD profile for d4-FOX-7 at $m/z = 30$ confirms the assignment. Nitric oxide also has the highest intensity signal in ReTOF-MS, and given that NO was among the least abundant species detected using QMS (only higher than NCCN), it is not surprising that QMS could not
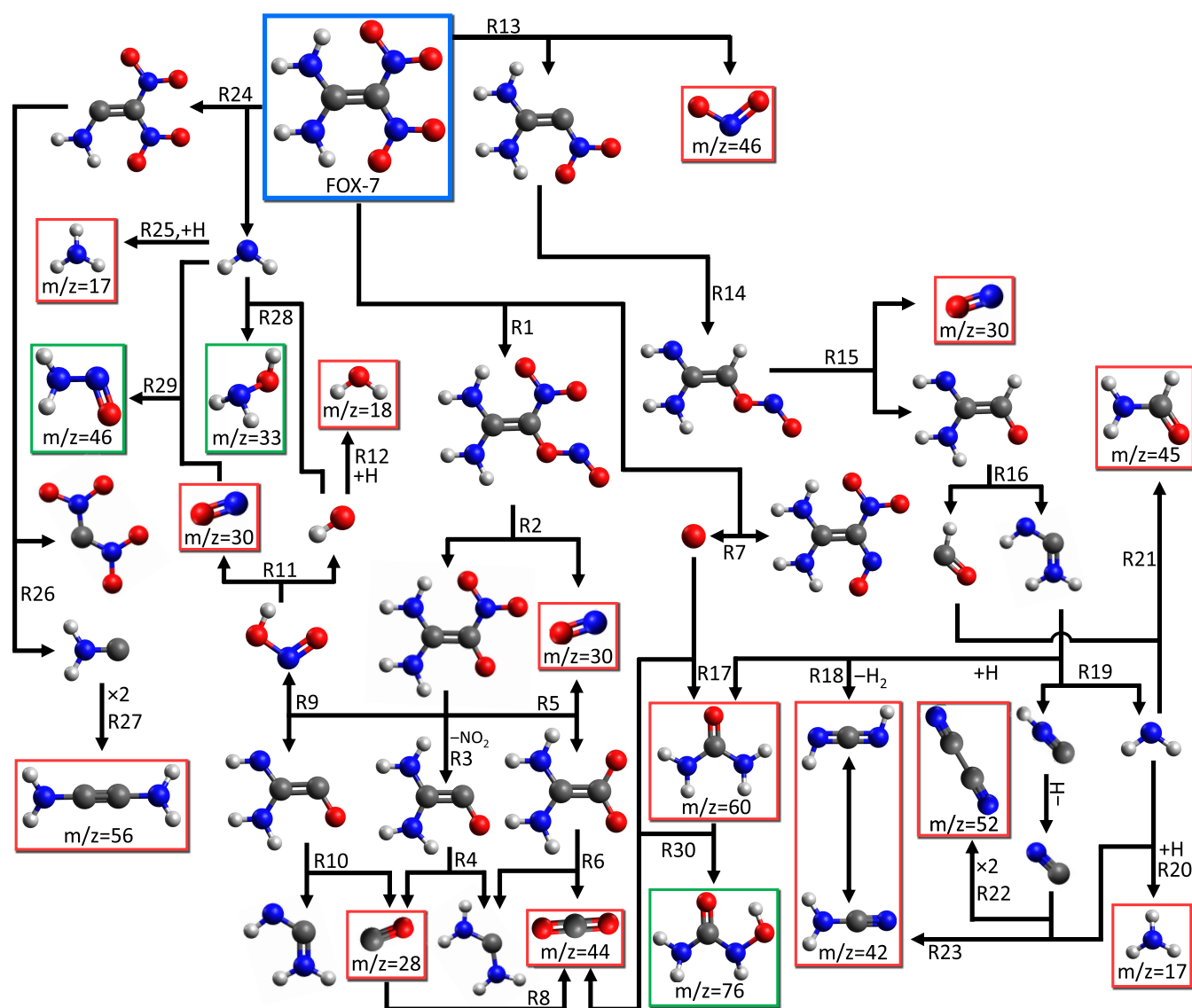
Figure 7. Reaction schemes from FOX-7 (top) showing decomposition pathways toward observed products (boxes with the mass-to-charge ratio). Products in red boxes were also observed during the irradiation with electrons,[48] while those in green boxes are newly observed in this study. The pathway for reaction 1 is labeled R1 and so forth.

detect the other molecules with ReTOF-MS profiles. The lowest mass-to-charge observed was $m/z = 17$ and matched the profile of $m/z = 20$ using d4-FOX-7, giving the assignment for ammonia (NH_3, IE = 10.07 eV),[58] which began subliming at 177 K and peaked at 207 and 240 K. Also at 177 K, the profile for $m/z = 33$ with the corresponding $m/z = 36$ profile in d4-FOX-7 began subliming with peaks at 212 and 232 K. This can be assigned to hydroxylamine (NH_2OH). The profile for $m/z = 46$ displays peaks caused by the sublimation of two distinct molecules. The first and most intense peak at 166 K closely aligns with a peak in d4-FOX-7 at $m/z = 46$, indicating no hydrogen atoms and the formula for nitrogen dioxide (NO_2). Note that NO_2 was not observed after the 532 and 355 nm photolysis, even though calculations of gas-phase FOX-7 predict that NO_2 should have formed at these energies. However, calculations that take into account the crystalline structure of FOX-7 correctly predicted the lack of detection after 532 nm photolysis, but a disagreement still existed for 355 nm photolysis. The detection of NO_2 with the current 202 nm

photolysis confirms that these photons have sufficient energy to overcome the discrepancy between the calculated energetics and those of the actual crystalline structure in order to initiate the predicted reactions. A higher temperature peak at 268 K matches the d4-FOX-7 profile at $m/z = 48$, meaning the molecule assigned to this peak has two hydrogen atoms. Two formulas satisfy these requirements: HCOOH (formic acid) and H_2N_2O (nitrosamine, NH_2NO). However, formic acid has an ionization energy of 11.0 eV and thus would not be ionized and detected with 10.49 eV photons, so this peak at $m/z = 46$ belongs to H_2N_2O. This example highlights the issues with assigning larger molecules because multiple possible formulas can satisfy a given mass-to-charge, even when deuterated experiments constrain the number of hydrogen atoms. Additional TPD profiles with multiple possible assignments occur at the following mass-to-charge ratios (with the corresponding profile from d4-FOX-7 in parentheses): 42 (44), 45 (48), 56 (60), 60 (64), and 76 (80). To assign these masses, previous experiments and calculations studying FOX-7

decomposition reactions must be considered, which is continued in the Discussion section.

4. DISCUSSION

By utilizing previous computational and experimental results, a detailed mechanistic discussion of the observed products is presented. A detailed discussion for $m/z = 30$ (NO) is included in the analysis of the 355 nm experiment,[17] while discussions of $m/z = 17$ (NH$_3$), 18 (H$_2$O), 28 (CO), 30 (NO), 42 (CH$_2$N$_2$), 44 (CO$_2$), 45 (CH$_3$NO), 46 (NO$_2$), 52 (NCCN), 56 (C$_2$H$_4$N$_2$), and 60 (CH$_4$N$_2$O) are presented with the electron irradiation experiment.[48] To summarize, irradiated FOX-7 may undergo nitro-to-nitrite isomerization (reaction 1, Figure 7 and Table S2), a critical first step toward many reactions and observed spectroscopically from 355 nm photolysis.[17] Nitric oxide (NO) is then produced from cleavage of the CO−NO bond (reaction 2), leaving the C(NH$_2$)$_2$C(O)NO$_2$ radical. The loss of the nitro group from the resulting fragment gives nitrogen dioxide (NO$_2$, $m/z = 46$) and C(NH$_2$)$_2$CO (reaction 3), which can further decompose to carbon monoxide (CO, $m/z = 28$) and the C(NH$_2$)$_2$ fragment (reaction 4). Returning to the C(NH$_2$)$_2$C(O)NO$_2$ radical, a second nitro-to-nitrite isomerization, followed by NO loss (reaction 5), results in C(NH$_2$)$_2$CO$_2$. Breakage of the C=C bond produces carbon dioxide (CO$_2$, $m/z = 44$) and C(NH$_2$)$_2$ (reaction 6). The generation of atomic oxygen from a FOX-7 molecule (reaction 7) can react with carbon monoxide as an alternate path to CO$_2$ (reaction 8)—a reaction observed in carbon monoxide ice.[60] In addition to reaction 3 and reaction 5, the C(NH$_2$)$_2$C(O)NO$_2$ radical can undergo a hydrogen shift and then split into the NH$_2$C(NH)-CO and HONO fragments (reaction 9). Carbon monoxide is produced from the C=C bond cleavage of NH$_2$C(NH)CO (reaction 10), while the HONO fragment can decompose to NO and the hydroxyl radical (OH, reaction 11). The addition of hydrogen to OH, for example, through radical−radical recombination or through abstraction of a hydrogen atom from FOX-7, results in water (H$_2$O, $m/z = 18$, reaction 12).

These mechanisms highlight the importance of an initial nitro-to-nitrite isomerization. This isomerization can also occur in a later step; for example, FOX-7 can initially lose a nitro group to form NO$_2$ and the C(NH$_2$)$_2$CNO$_2$ radical (reaction 13), which can undergo a hydrogen shift and nitro-to-nitrite isomerization to NH$_2$C(NH)CHONO (reaction 14). The loss of NO from this fragment gives NH$_2$C(NH)CHO (reaction 15). Further decomposition at the C=C bond gives the HCO and C(NH$_2$)$_2$ fragments (reaction 16). The C(NH$_2$)$_2$ fragment was also generated from reactions 4 and 6 and serves as a significant intermediate toward several products. The recombination of C(NH$_2$)$_2$ with an oxygen atom could form urea (NH$_2$C(O)NH$_2$, $m/z = 60$, reaction 17), while the loss of two hydrogens from C(NH$_2$)$_2$ creates C(NH)$_2$ (reaction 18) and its more stable tautomer, cyanamide (NH$_2$CN, $m/z = 42$). The C(NH$_2$)$_2$ fragment can also dissociate with hydrogen isocyanide (HNC) and the amino radical (NH$_2$, reaction 19). Hydrogen addition to NH$_2$ gives ammonia (NH$_3$, $m/z = 17$, reaction 20), while radical−radical recombination of NH$_2$ and HCO from reaction 16 produces formamide (NH$_2$CHO, $m/z = 45$, reaction 21). Hydrogen loss from HNC generates the cyano radical (CN), which can either combine with another cyano radical to form cyanogen (NCCN, $m/z = 52$, reaction 22) or with an amino radical, resulting in cyanamide (NH$_2$CN, $m/z = 42$, reaction 23). The amino radical could

also cleave directly from a FOX-7 molecule as an initial first step (reaction 24), which serves as a more direct route to ammonia formation with the addition of a hydrogen atom (reaction 25). The counter fragment, NH$_2$CC(NO$_2$)$_2$, can further decompose to C(NO$_2$)$_2$ and CNH$_2$ (reaction 26), and the recombination of two CNH$_2$ fragments produces diaminoacetylene (NH$_2$CCNH$_2$, $m/z = 56$, reaction 27).

In addition to these products, signals at $m/z = 33$, 46, and 76 were also observed after 202 nm irradiation but were not detected after electron irradiation. Each of these masses can be assigned to products capable of forming by the recombination of two intermediate species identified in computational studies and presented previously. As mentioned in the Results, a formula with $m/z = 33$ and three hydrogen atoms can be uniquely assigned to hydroxylamine (NH$_2$OH), which can be formed by radical−radical recombination of amino (NH$_2$) and hydroxyl (OH) radicals. The route to amino radical production is through the separation of the amine group from FOX-7 (reaction 24), which requires 461 kJ mol^{-1} (4.78 eV) of energy. A 202 nm photon (6.14 eV) has sufficient energy to cleave this carbon−nitrogen bond, while the 355 nm (3.49 eV) photons used in previous studies are insufficient and explain why amine-based products were not observed after 355 nm irradiation. The formation of the hydroxyl radical necessarily involves a hydrogen atom transfer from an amine (NH$_2$) group to oxygen from the nitro (NO$_2$) group. This can proceed after nitro-to-nitrite isomerization (reaction 1), which stabilizes the molecule by 18 kJ mol^{-1} after passing through a 273 kJ mol^{-1} transition state, and subsequent loss of nitric oxide (reaction 2, 3 kJ mol^{-1}). After hydrogen transfer through a 16 kJ mol^{-1} transition state to the nitro group and separation of the resulting HONO group (reaction 9, 112 kJ mol^{-1}), the nitrous acid (HONO) molecule can decompose into nitric oxide (NO) and the hydroxyl radical (OH, reaction 11, 197 kJ mol^{-1}). Hydroxylamine (NH$_2$OH) is thus formed by the recombination of the amino and hydroxyl radicals (reaction 28), which is exoergic by 260 kJ mol^{-1},[58] and serves as a transitional oxidation compound, providing a missing link between reduced ammonia (NH$_3$) and oxidized nitric oxide (NO) and nitrogen dioxide (NO$_2$). An alternative pathway to hydroxylamine was found in electron-irradiated ices of ammonia and molecular oxygen in which suprathermal atomic oxygen (^{1}D) was inserted into the nitrogen−hydrogen bond of ammonia.[61] This is the first experimental detection of hydroxylamine as a decomposition product of FOX-7 and serves as an archetype linking experimental findings with theoretical calculations that can be achieved using photolytic methods to probe individual reactions on a molecular level.

The reaction scheme through reaction 11 can also be utilized to explain the formation of H$_2$N$_2$O, which is observed as the second peak (268 K) in the $m/z = 46$ TPD profile that matches the $m/z = 48$ peak using d4-FOX-7. Two isomers with this formula include the highly unstable cyclic oxadiaziridine (c-NHNHO) and the more common nitrosamine (NH$_2$NO), which can be generated from the reaction of the amino radical (NH$_2$) and nitric oxide (NO).[62] Nitric oxide can form after nitro-to-nitrate isomerization, such as in reactions 2 or 14, or from the decomposition of nitrous acid (HONO) in reaction 11, while the amino radical results from any cleavage of an unaltered amine group from the carbon atom, including reaction 24. Recombination of nitric oxide, a stable radical, with the amino radical, gives the closed-shell nitrosamine (NH$_2$NO, reaction 29) and is exoergic by 195 kJ mol^{-1}.[58] Like

hydroxylamine, nitrosamine is a relatively simple molecule that has not been detected as a decomposition product of FOX-7, thus expanding the possibilities of potential higher-order products.

The final mass-to-charge ratio to evaluate is $m/z = 76$. The corresponding TPD profile for d4-FOX-7 at $m/z = 80$ greatly reduces the possible assignments to those with four hydrogen atoms: H_4N_4O, C_6H_4, $CH_4N_2O_2$, and $C_2H_4O_3$. The H_4N_4O formula has never been experimentally observed, while hydrocarbons, such as C_6H_4, have never been identified experimentally nor computationally in the decomposition of FOX-7, and thus these will not be considered further. Moreover, isomers of $C_2H_4O_3$, including glycolic acid ($HOCH_2COOH$) and peracetic acid ($CH_3C(O)OOH$), require hydrogenated forms of carbon ($-CH_2-$ and $-CH_3$, respectively) never observed in FOX-7 decomposition studies. Thus, the most plausible assignment to $m/z = 76$ is $CH_4N_2O_2$. Unfortunately, numerous isomers belong to this formula, and determining the particular isomer(s) contributing to $m/z = 76$ would be unfeasible. However, using the proposed products at lower mass-to-charge ratios in this and previous studies, hydroxyurea ($NH_2C(O)NHOH$) can be assigned as a plausible identification. The formation of hydroxyurea follows from the diaminocarbene fragment ($C(NH_2)_2$), which results from several reaction pathways involving carbon−carbon bond cleavage, such as reactions 4 and 16. Diaminocarbene can combine with atomic oxygen, which is liberated from FOX-7 after breaking a nitrogen−oxygen bond of 344 kJ mol^{-1}, to form urea at $m/z = 60$ (($NH_2)_2CO$, reaction 17). The reaction of urea with an additional oxygen atom, which is expected to insert barrierlessly in the excited ^1D state,[63−67] would form hydroxyurea (reaction 30) if inserted into one of the four nitrogen−hydrogen bonds of urea. Previous studies of FOX-7, both computational and experimental, have not identified a product at $m/z = 76$ as this molecule is much larger than those typically encountered with FOX-7 degradation and thus a comparison of this assignment to other works is not possible. This highlights the need for further studies, especially theoretical ones, that consider reaction pathways toward higher-order products.

5. CONCLUSIONS

The 202 nm photolysis of solid FOX-7 at 5 K generated products from an intermediate irradiation dose between lower-energy photons (355 and 532 nm) and higher-energy electrons. The 202 nm and electron irradiation[48] observed the same five products using quadrupole mass spectrometry: water (H_2O), carbon monoxide (CO), nitric oxide (NO), carbon dioxide (CO_2), and cyanogen (NCCN). This agreement highlights the role of these molecules as ultimate decomposition products of FOX-7, given the high abundance necessary for detection using QMS. Carbon monoxide and carbon dioxide are especially notable because FOX-7 does not contain a carbon−oxygen bond and thus these compounds indicate near-complete combustion of photolyzed molecules. The experiments utilizing 355 and 532 nm photons predominantly observed molecular oxygen (O_2),[17] which branded FOX-7 as an energetic material capable of providing its own oxidant. At higher photon/electron energies, O_2 was not observed, but instead, the most abundant molecules were the classical combustion products of a hydrocarbon and oxygen, suggesting that the increased irradiation energy not only generated oxygen but provided sufficient energy to further

react and decompose FOX-7 such as to hydroxylamine (NH_2OH). Water served as the next most abundant compound detected and could easily form from the dissociation of oxygen (or hydroxyl after a hydrogen shift) from FOX-7 and the acquisition of additional hydrogen from the matrix. Thus, the three most abundant products of 202 nm irradiation (CO, CO_2, H_2O) and the most abundant of 355 and 532 nm photolysis (O_2) all originate from the release of oxygen, with the final product determined by the degree of excess energy. After these products, nitric oxide had the highest quantity and was observed with both 355 and 202 nm photolysis. Nitric oxide results after nitro-to-nitrite isomerization, which is an important first step toward higher-order decomposition products. Finally, cyanogen represents the most prominent species of detected nitriles that have been observed in other studies, as well as this experiment, in the form of infrared absorptions (CN^-, OCN^-, $\nu(CN)$) and ReTOF-detected products such as cyanamide (NH_2CN). ReTOF-MS also detected three products after 202 nm photolysis, not observed by other irradiation energies. The formula for hydroxylamine (NH_3O) is explicitly confirmed at $m/z = 33$, along with nitrosamine (H_2N_2O) at $m/z = 46$, which cannot be formic acid (HCOOH) due to having an ionization energy (11.0 eV) above the ionizing photon energy (10.49 eV). Finally, the signal at $m/z = 76$ could be assigned to several formulas and isomers, but by utilizing previous experimental and computational results, the formula $CH_4N_2O_2$ is proposed and represented by the hydroxyurea isomer ($NH_2C(O)$-NHOH). These three products—hydroxylamine, nitrosamine, and $CH_4N_2O_2$—are new experimentally detected decomposition products of FOX-7 and encourage further experimental and theoretical studies into higher-order products. The latter two results pose both a problem and a solution. The use of d4-FOX-7 constrained the formula for $m/z = 76$ to four hydrogen atoms, but this did not uniquely identify one molecular formula, so additional experiments using other isotopes, such as carbon-13, would assist in confirming the proposed assignments. However, once a formula is explicitly defined, determining the specific isomer is informative. This can be accomplished in a manner similar to excluding the formic acid assignment due to its high ionization energy. The ionization energies for isomers belonging to each molecular formula can be calculated, and the experiments can be repeated using tunable photoionization to unambiguously determine the isomer responsible for the observed signal.[52] This further highlights the benefits of computations and experiments working in tandem to investigate energetic materials, which has been utilized here and in previous works to probe calculated reaction energies using experimental results and to confirm theoretical predictions, which are often limited to small molecules in the gas phase, with condensed-phase experiments designed to inhibit thermal reactions.

■ ASSOCIATED CONTENT

Ⓢ Supporting Information

The Supporting Information is available free of charge at https://pubs.acs.org/doi/10.1021/acs.jpca.3c03215.

> Infrared assignments of FOX-7 from 600 to 6000 cm^{-1}, TPD profile of $m/z = 45$ using QMS, and energetics of reactions in Figure 7 (PDF)

■ AUTHOR INFORMATION

Corresponding Author

Ralf I. Kaiser − *Department of Chemistry and W. M. Keck Research Laboratory in Astrochemistry, University of Hawaii, Honolulu, Hawaii 96822, United States;* ◉ orcid.org/0000-0002-7233-7206; Email: ralfk@hawaii.edu

Authors

Andrew M. Turner − *Department of Chemistry and W. M. Keck Research Laboratory in Astrochemistry, University of Hawaii, Honolulu, Hawaii 96822, United States*

Joshua H. Marks − *Department of Chemistry and W. M. Keck Research Laboratory in Astrochemistry, University of Hawaii, Honolulu, Hawaii 96822, United States*

Jasmin T. Lechner − *Department of Chemistry, Ludwig-Maximilian University of Munich, München 81377, Germany;* ◉ orcid.org/0000-0002-8391-8604

Thomas M. Klapötke − *Department of Chemistry, Ludwig-Maximilian University of Munich, München 81377, Germany;* ◉ orcid.org/0000-0003-3276-1157

Rui Sun − *Department of Chemistry, University of Hawaii, Honolulu, Hawaii 96822, United States;* ◉ orcid.org/0000-0003-0638-1353

Complete contact information is available at:
https://pubs.acs.org/10.1021/acs.jpca.3c03215

Notes

The authors declare no competing financial interest.

■ REFERENCES

(1) Latypov, N. V.; Bergman, J.; Langlet, A.; Wellmar, U.; Bemm, U. Synthesis and Reactions of 1,1-Diamino-2,2-Dinitroethylene. *Tetrahedron* **1998**, *54*, 11525−11536.

(2) Fried, L. E.; Manaa, M. R.; Lewis, J. P. *Overviews of Recent Research on Energetic Materials*; Shaw, R. W.; Brill, T. B.; Thompson, D. L., Eds.; World Scientific Publishing: Singapore, 2005; pp 275−301.

(3) Oxley, J. C. *Theoretical and Computational Chemistry*; Politzer, P.; Murray, J. S., Eds.; Elsevier: New York, 2003; Vol. 12, pp 5−48.

(4) Kozak, G. D. Factors Augmenting the Detonability of Energetic Materials. *Propellants, Explos., Pyrotech.* **2005**, *30*, 291−297.

(5) Singh, S. K.; Vuppuluri, V.; Son, S. F.; Kaiser, R. I. Investigating the Photochemical Decomposition of Solid 1,3,5-Trinitro-1,3,5-Triazinane (RDX). *J. Phys. Chem. A* **2020**, *124*, 6801−6823.

(6) Singh, S. K.; La Jeunesse, J.; Vuppuluri, V.; Son, S. F.; Sun, B.-J.; Chen, Y.-L.; Chang, A. H. H.; Mebel, A. M.; Kaiser, R. I. The Elusive Ketene (H₂CCO) Channel in the Infrared Multiphoton Dissociation of Solid 1,3,5-Trinitro-1,3,5-Triazinane (RDX). *ChemPhysChem* **2020**, *21*, 837−842.

(7) Sikder, A. K.; Sikder, N. A Review of Advanced High Performance, Insensitive and Thermally Stable Energetic Materials Emerging for Military and Space Applications. *J. Hazard. Mater.* **2004**, *112*, 1−15.

(8) Badgujar, D. M.; Talawar, M. B.; Asthana, S. N.; Mahulikar, P. P. Advances in Science and Technology of Modern Energetic Materials: An Overview. *J. Hazard. Mater.* **2008**, *151*, 289−305.

(9) Adams, G. F.; Shaw, R. W. Chemical Reactions in Energetic Materials. *Annu. Rev. Phys. Chem.* **1992**, *43*, 311−340.

(10) Brill, T. B.; James, K. J. Kinetics and Mechanisms of Thermal Decomposition of Nitroaromatic Explosives. *Chem. Rev.* **1993**, *93*, 2667−2692.

(11) Behrens, R. *Overviews of Recent Research on Energetic Materials*; Shaw, R. W.; Brill, T. B.; Thompson, D. L., Eds.; World Scientific Publishing: Singapore, 2005; pp 29−73.

(12) Majano, G.; Mintova, S.; Bein, T.; Klapötke, T. M. Confined Detection of High-Energy-Density Materials. *J. Phys. Chem. C* **2007**, *111*, 6694−6699.

(13) Mathieu, D. Mateo: A Software Package for the Molecular Design of Energetic Materials. *J. Hazard. Mater.* **2010**, *176*, 313−322.

(14) Shteinberg, A. S.; Berlin, A. A.; Denisaev, A. A.; Mukasyan, A. S. Kinetics of Fast Reactions in Condensed Systems: Some Recent Results (an Autoreview). *Int. J. Self-Propag. High-Temp. Synth.* **2011**, *20*, 259−265.

(15) Luo, Y.; Kang, C.; Kaiser, R.; Sun, R. The Potential Energy Profile of the Decomposition of 1,1-Diamino-2,2-Dinitroethylene (Fox-7) in the Gas Phase. *Phys. Chem. Chem. Phys.* **2022**, *24*, 26836−26847.

(16) Gindulyte, A.; Massa, L.; Huang, L.; Karle, J. *Theoretical and Computational Chemistry*; Politzer, P.; Murray, J. S., Eds.; Elsevier: New York, 2003; Vol. 12, pp 91−109.

(17) Turner, A. M.; Luo, Y.; Marks, J. H.; Sun, R.; Lechner, J. T.; Klapötke, T. M.; Kaiser, R. I. Exploring the Photochemistry of Solid 1,1-Diamino-2,2-Dinitroethylene (FOX-7) Spanning Simple Bond Ruptures, Nitro-to-Nitrite Isomerization, and Nonadiabatic Dynamics. *J. Phys. Chem. A* **2022**, *126*, 4747−4761.

(18) Booth, R. S.; Butler, L. J. Thermal Decomposition Pathways for 1,1-Diamino-2,2-Dinitroethene (Fox-7). *J. Chem. Phys.* **2014**, *141*, No. 134315.

(19) Guan, Y.; Zhu, X.; Gao, Y.; Ma, H.; Song, J. Initial Thermal Decomposition Mechanism of $(NH_2)_2C=C(NO_2)(ONO)$ Revealed by Double-Hybrid Density Functional Calculations. *ACS Omega* **2021**, *6*, 15292−15299.

(20) Kiselev, V. G.; Gritsan, N. P. Unexpected Primary Reactions for Thermolysis of 1,1-Diamino-2,2-Dinitroethylene (FOX-7) Revealed by Ab Initio Calculations. *J. Phys. Chem. A* **2014**, *118*, 8002−8008.

(21) Yuan, B.; Yu, Z.; Bernstein, E. R. Initial Decomposition Mechanism for the Energy Release from Electronically Excited Energetic Materials: FOX-7 (1,1-Diamino-2,2-Dinitroethene). *J. Chem. Phys.* **2014**, *140*, No. 074708.

(22) Kimmel, A. V.; Sushko, P. V.; Shluger, A. L.; Kuklja, M. M. Effect of Charged and Excited States on the Decomposition of 1,1-Diamino-2,2-Dinitroethylene Molecules. *J. Chem. Phys.* **2007**, *126*, No. 234711.

(23) Politzer, P.; Concha, M. C.; Grice, M. E.; Murray, J. S.; Lane, P. Computational Investigation of the Structures and Relative Stabilities of Amino/Nitro Derivatives of Ethylene. *J. Mol. Struct.: THEOCHEM* **1998**, *452*, 75−83.

(24) Türker, L.; Varış, S. Effects of Epoxidation and Nitration on Ballistic Properties of FOX-7—a DFT Study. *Z. Anorg. Allg. Chem.* **2013**, *639*, 982−987.

(25) Rashkeev, S. N.; Kuklja, M. M.; Zerilli, F. J. Electronic Excitations and Decomposition of 1,1-Diamino-2,2-Dinitroethylene. *Appl. Phys. Lett.* **2003**, *82*, 1371−1373.

(26) Zheng, Z.; Xu, J.; Zhao, J. First-Principles Studies on the Thermal Decomposition Behavior of FOX-7. *High Pressure Res.* **2010**, *30*, 301−309.

(27) Zong, H.; Huang, Y.; Shu, Y.; Wang, X. *Theoretical Study on the Initial Thermal Decomposition and Catalysis Effects of NO2 on FOX-7*; Hanneng Cailiao, 2006; Vol. 14, pp 425−428.

(28) Liu, Y.; Li, F.; Sun, H. Thermal Decomposition of FOX-7 Studied by Ab Initio Molecular Dynamics Simulations. *Theor. Chem. Acc.* **2014**, *133*, 1567.

(29) Ma, Y.; Lv, M.; Shang, F.; Zhang, C.; Liu, J.; Zhou, P. Mechanistic Investigation on the Initial Thermal Decomposition of Energetic Materials FOX-7 and RDX in the Crystal and Gas Phase: An MM/DFT-Based Oniom Calculation. *J. Phys. Chem. A* **2022**, *126*, 1666−1673.

(30) Jones, D.; Vachon, M.; Wang, R.; Kwok, Q. In *Preliminary Studies on the Thermal Properties of FOX-7*, Proceedings of the

NATAS Annual Conference on Thermal Analysis and Applications 32nd, 2004; pp 1−105.

(31) Jin, P.-G.; Chang, H.; Chen, Z.-Q. *Studies on Kinetics and Mechanisms of Thermal Decomposition of 1,1-Diamino-2,2-Dinitroethylene (FOX-7)*; Baozha Yu Chongji, 2006; Vol. 26, p 528.

(32) Zhang, J.-D.; Zhang, L.-L. Theoretical Study on the Mechanism of the Reaction of FOX-7 with OH and NO_2 Radicals: Bimolecular Reactions with Low Barrier During the Decomposition of FOX-7. *Mol. Phys.* 2017, *115*, 2951−2960.

(33) Bellamy, A. J. *High Energy Density Materials*; Klapötke, T. M., Ed.; Springer: Berlin, Heidelberg, 2007; pp 1−33.

(34) Jiang, L.; Fu, X.; Zhou, Z.; Zhang, C.; Li, J.; Qi, F.; Fan, X.; Zhang, G. Study of the Thermal Decomposition Mechanism of FOX-7 by Molecular Dynamics Simulation and Online Photoionization Mass Spectrometry. *RSC Adv.* 2020, *10*, 21147−21157.

(35) Yuan, W.-S.; Liu, Q.-J.; Hong, D.; Wei, D.; Liu, F.-S.; Wang, W.-P.; Liu, Z.-T. Raman Spectra and Vibrational Properties of FOX-7 under Pressure and Temperature: First-Principles Calculations. *Spectrochim. Acta, Part A* 2023, *293*, No. 122489.

(36) Banik, S.; Yadav, A. K.; Kumar, P.; Ghule, V. D.; Dharavath, S. Unfolding the Chemistry of Fox-7: Unique Energetic Material and Precursor with Numerous Possibilities. *Chem. Eng. J.* 2021, No. 133378.

(37) Kushtaev, A. A.; Yudin, N. V.; Kondakova, N. N.; Ilicheva, N. N.; Vu, T. Q.; Zbarskiy, V. L. Investigation of FOX-7 Polymorphs: New Polymorphs-ϵ and ζ. *ChemistrySelect* 2021, *6*, 12562−12570.

(38) Sinditskii, V. P.; Kushtaev, A. A.; Yudin, N. V.; Levshenkov, A. I.; Kondakova, N. N.; Alekseeva, M. A. 1, 1-Diamino-2, 2-Dinitroethylene: The Riddles of Thermal Decomposition and Combustion. *J. Phys. Chem. Solids* 2023, *177*, No. 111275.

(39) Li, J.; Zhou, T.; Chen, J.; Wang, X.; Wang, Y.; Liu, W.; Zhang, X.; Li, Z.; Chen, X.; Han, J.; Kim, C. K. Theoretical Studies on 2,3,5,6-Tetra(1H-Tetrazol-5-yl)Pyrazine and 1,1-Diamino-2,2-Dinitroethylene Blending System. *J. Mol. Graphics Modell.* 2022, *116*, No. 108235.

(40) Ghosh, M.; Sikder, A. K.; Banerjee, S.; Talawar, M. B.; Sikder, N. Preparation of Reduced Sensitivity Co-Crystals of Cyclic Nitramines Using Spray Flash Evaporation. *Def. Technol.* 2020, *16*, 188−200.

(41) Wang, B.; Jiao, F.; Xu, R.; Li, H. Construction of Nano-Sized FOX-7/ZIF-8 Composites for Fast Decomposition and Reduced Sensitivity. *RSC Adv.* 2023, *13*, 1862−1866.

(42) Lal, S.; Staples, R. J.; Jean'ne, M. S. FOX-7 Based Nitrogen Rich Green Energetic Salts: Synthesis, Characterization, Propulsive and Detonation Performance. *Chem. Eng. J.* 2023, *452*, No. 139600.

(43) Krisyuk, B. E.; Sypko, T. M. Mechanism of Thermolysis of Hydrazino-Dinitroethylenes. *Comput. Theor. Chem.* 2022, *1211*, No. 113662.

(44) Shang, F.; Wang, T.; Ma, Y.; Lv, M. Theoretical Study on Several Important Decomposition Paths of FOX-7 and Its Derivatives. *Comput. Theor. Chem.* 2022, *1217*, No. 113895.

(45) Nazin, G. M.; Dubikhin, V.; Kazakov, A.; Nabatova, A.; Krisyuk, B.; Volkova, N.; Shastin, A. Kinetics of the Decomposition of 1,1-Diamino-2,2-Dinitroethylene (FOX-7). Part 4: Comparison of the Decomposition Reactions of FOX-7 and Its Diazacyclic Derivatives. *Russ. J. Phys. Chem. B* 2022, *16*, 308−315.

(46) Xue, M.; Li, Y.; He, C.; Pang, S. Design and Theoretical Studies of FOX-7-Like Novel Energetic Compounds. *New J. Chem.* 2023, *47*, 919−930.

(47) Ghanta, S. Design of Derivatives of FOX-7-Based New Four-Member Heterocyclic Insensitive High Energy Density Molecules: A Theoretical Prospectives. *J. Mol. Model.* 2023, *29*, 18.

(48) Turner, A. M.; Marks, J. H.; Luo, Y.; Lechner, J. T.; Klapötke, T. M.; Sun, R.; Kaiser, R. I. Electron-Induced Decomposition of Solid 1,1-Diamino-2,2-Dinitroethylene (FOX-7) at Cryogenic Temperatures. *J. Phys. Chem. A* 2023, *127*, 3390−3401.

(49) Latypov, N. V.; Johansson, M.; Holmgren, E.; Sizova, E. V.; Sizov, V. V.; Bellamy, A. J. On the Synthesis of 1,1-Diamino-2,2-

Dinitroethene (FOX-7) by Nitration of 4,6-Dihydroxy-2-Methylpyrimidine. *Org. Process Res. Dev.* 2007, *11*, 56−59.

(50) Astrat'ev, A. A.; Dashko, D. V.; Mershin, A. Y.; Stepanov, A. I.; Urazgil'deev, N. A. Some Specific Features of Acid Nitration of 2-Substituted 4,6-Dihydroxypyrimidines. Nucleophilic Cleavage of the Nitration Products. *Russ. J. Org. Chem.* 2001, *37*, 729−733.

(51) Jones, B. M.; Kaiser, R. I. Application of Reflectron Time-of-Flight Mass Spectroscopy in the Analysis of Astrophysically Relevant Ices Exposed to Ionization Radiation: Methane (CH_4) and D_4-Methane (CD_4) as a Case Study. *J. Phys. Chem. Lett.* 2013, *4*, 1965−1971.

(52) Turner, A. M.; Kaiser, R. I. Exploiting Photoionization Reflectron Time-of-Flight Mass Spectrometry to Explore Molecular Mass Growth Processes to Complex Organic Molecules in Interstellar and Solar System Ice Analogs. *Acc. Chem. Res.* 2020, *53*, 2791−2805.

(53) Hilbig, R.; Wallenstein, R. Narrowband Tunable Vuv Radiation Generated by Nonresonant Sum-and Difference-Frequency Mixing in Xenon and Krypton. *Appl. Opt.* 1982, *21*, 913−917.

(54) Klapötke, T. M.; Krumm, B.; Lechner, J. T.; Stierstorfer, J. Investigation of Deuterated FOX-7−Changes in Structural Behavior and Energetic Characteristics after Deuteration under Ambient Conditions. *Dalton Trans.* 2022, *51*, 5788−5791.

(55) Schmid, M.; Parkinson, G. S.; Diebold, U. Analysis of Temperature-Programmed Desorption via Equilibrium Thermodynamics. *ACS Phys. Chem. Au* 2023, *3*, 44−62.

(56) *Atomic Weights and Isotopic Compositions with Relative Atomic Masses*; NIST Physical Measurement Laboratory. https://www.nist.gov/pml/atomic-weights-and-isotopic-compositions-relative-atomic-masses (accessed May 5, 2023).

(57) Bennett, C. J.; Jamieson, C.; Mebel, A. M.; Kaiser, R. I. Untangling the Formation of the Cyclic Carbon Trioxide Isomer in Low Temperature Carbon Dioxide Ices. *Phys. Chem. Chem. Phys.* 2004, *6*, 735−746.

(58) *NIST Standard Reference Database Number 69*; National Institute of Standards and Technology. https://webbook.nist.gov/chemistry/ (accessed May 5, 2023).

(59) Argonne National Laboratory. Active Thermochemical Tables. https://atct.anl.gov/ (accessed May 5, 2023).

(60) Bennett, C. J.; Jamieson, C. S.; Kaiser, R. I. An Experimental Investigation of the Decomposition of Carbon Monoxide and Formation Routes to Carbon Dioxide in Interstellar Ices. *Astrophys. J., Suppl. Ser.* 2009, *182*, 1.

(61) Tsegaw, Y. A.; Góbi, S.; Förstel, M.; Maksyutenko, P.; Sander, W.; Kaiser, R. I. Formation of Hydroxylamine in Low-Temperature Interstellar Model Ices. *J. Phys. Chem. A* 2017, *121*, 7477−7493.

(62) López-Rodríguez, R.; McManus, J. A.; Murphy, N. S.; Ott, M. A.; Burns, M. J. Pathways for N-Nitroso Compound Formation: Secondary Amines and Beyond. *Org. Process Res. Dev.* 2020, *24*, 1558−1585.

(63) Zhu, C.; Kleimeier, N. F.; Turner, A. M.; Singh, S. K.; Fortenberry, R. C.; Kaiser, R. I. Synthesis of Methanediol [$CH_2(OH)_2$]: The Simplest Geminal Diol. *Proc. Natl. Acad. Sci. U.S.A.* 2022, *119*, No. e2111938119.

(64) Singh, S. K.; Zhu, C.; La Jeunesse, J.; Fortenberry, R. C.; Kaiser, R. I. Experimental Identification of Aminomethanol (NH_2CH_2OH)—the Key Intermediate in the Strecker Synthesis. *Nat. Commun.* 2022, *13*, No. 375.

(65) Ennis, C.; Yuan, H.; Sibener, S.; Kaiser, R. I. On the Chemical Processing of Hydrocarbon Surfaces by Fast Oxygen Ions. *Phys. Chem. Chem. Phys.* 2011, *13*, 17870−17884.

(66) Zheng, W.; Jewitt, D.; Kaiser, R. I. Formation of Hydrogen, Oxygen, and Hydrogen Peroxide in Electron-Irradiated Crystalline Water Ice. *Astrophys. J.* 2006, *639*, 534−548.

(67) Bennett, C. J.; Osamura, Y.; Lebar, M. D.; Kaiser, R. I. Laboratory Studies on the Formation of Three C_2H_4O Isomers—Acetaldehyde (CH_3CHO), Ethylene Oxide (C-C_2H_4O), and Vinyl Alcohol (CH_2CHOH)—in Interstellar and Cometary Ices. *Astrophys. J.* 2005, *634*, 698−711.